



# Engineering aspects of microwave axion generation and detection experiments using RF cavities

F. Caspers CERN-AB-RF

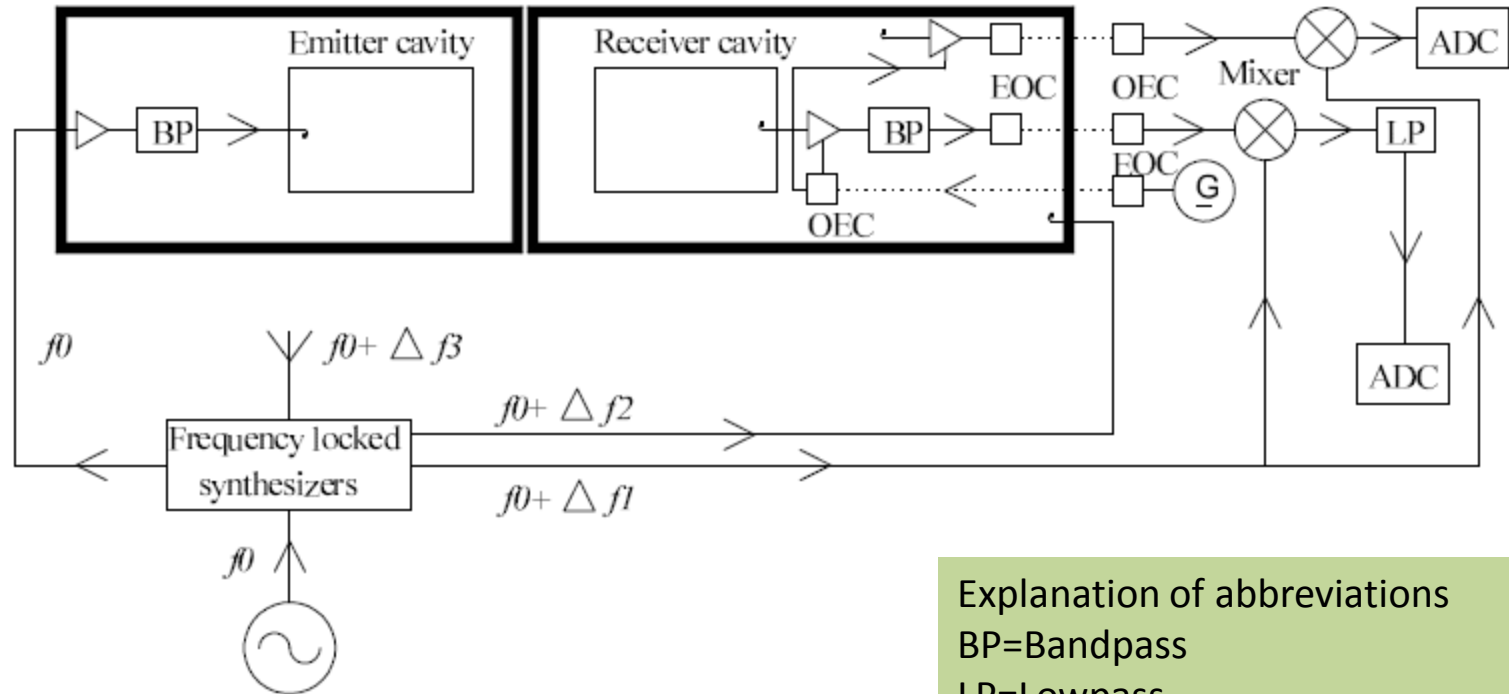
- Outline
- A microwave (axion) transmitter and receiver cavity set-up with high electromagnetic isolation
  - The “box in a box” concept with permanent control of RF leakage
  - Signal detection methods with very narrow observation bandwidth
- Rectangular waveguide  $TE_{10n}$  resonator in a LHC magnet
  - The transmitter cavity
  - The receiver cavity
- Axion radiation patterns (antenna diagram)
- Conclusion and outlook

## Two Cavity setup with very high isolation (1)

- A crucial ingredient for the experiment is to achieve sufficient shielding. For the intended sensitivity one has to achieve roughly a shielding of 300 dB (a factor  $10^{-30}$  in power) between the emitter and the receiver cavity. In order to provide sound data, testing of the shielding is mandatory, since we must be absolutely sure, that we are not fooled by simple electromagnetic leakage and or ambient electromagnetic noise
- As we cannot keep the ambient electromagnetic noise (cell phones, radio and TV stations etc) below a certain level, the more critical part will be on the receiver side.
- For the transmitter leakage a good reference level is the ambient electromagnetic parasitics level which is usually many orders of magnitude above the thermal noise level.

# Two Cavity setup with very high isolation (2)

The “box in a box concept”



**Feasibility, engineering aspects and physics reach of microwave cavity experiments searching for hidden photons and axions**

Published in JINST, Nov 16, 2009

F. Caspers,<sup>a</sup> J. Jaeckel<sup>b,1</sup> and A. Ringwald<sup>c</sup>

Explanation of abbreviations

BP=Bandpass

LP=Lowpass

ADC=Analog digital converter

OEC=Optical/electric converter

EOC=Electric optical converter

G=Generator (DC power source)

$\Delta f_1, \Delta f_2, \Delta f_3 < 20 \text{ KHz}$

## Two Cavity setup with very high isolation (3)

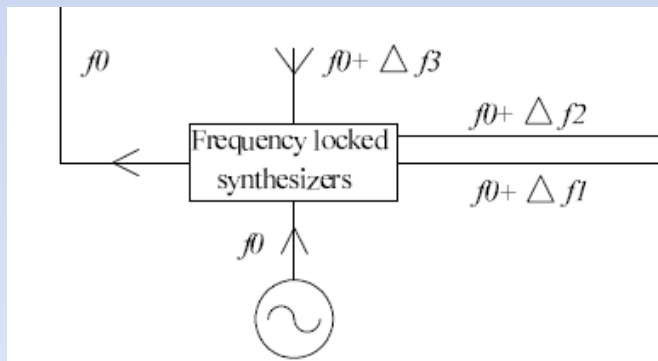
- One can obtain **AND MEASURE** realistically and in a straightforward manner a shielding value of about 100 dB in a single shell (box) by conventional means in the RF and microwave range. (of course higher values are possible).
- There are many examples for this like stochastic cooling systems but also all kind of modern microwave electronics and RF systems in particle accelerators.
- For higher requirements the “box in the box “concept can be applied..and if necessary extended to the “box in a box in a box..”
- However between those boxes (shielding shells which are usually demountable and not soldered) we need **ON-LINE** diagnostics showing, that this shielding performance is really maintained (degradation possible due to bad and ageing contacts) over the full lifetime of the experiment.

## Two Cavity setup with very high isolation (4)

- We have to transport signals and small amounts of DC power for preamplifiers and signal converters through those shells (receiver side) without degrading the performance of the shielding.
- Very likely the ONLY reliable way for this is using optical transmission but of RF/microwave signals but also of getting in a few Watt of DC power for feeding small signal amplifiers.
- Such DC power transmission using optical fibers (with LEDs at one end and photocells on the other side) and has been developed about 30 years ago to supply DC power to small electronic units on high voltage potential in HV transmission systems.
- Commercial systems for optical fiber based DC power transmission (5 Watt) are available from industry but there is a question mark about how well they would work at cryo temperatures and/ or in very strong magnetic fields

## Two Cavity setup with very high isolation (5)

- As for the transmitter side one cannot apply the same concept as for the receiver since we would like to feed several 10 Watt or maybe even more than 100 Watt average power (limited by the cryo system, in case a cryo system has to be used) into the transmitter cavity.
- Thus we have to do the best shielding which can be achieved with conventional means and need to monitor the residual RF leakage radiation by means of some antenna in the lab where the experiment is set up. Typically even with RF powers around 100 kW the residual radiation level can be kept around micro-Watts (which is still more than 10 orders magnitude above the thermal noise level for 1 Hz bandwidth)



That's why we emit into the lab deliberately a frequency (test tone at very low power around microwatts) at  $f_0 + \Delta f_3$  close to our signal  $f_0$  in order to be able to quantify any potential leakage between the first and second shell of the receiver setup.

# Two Cavity setup with very high isolation (6)

Example for a commercially available power transmission system on fiber



PHOTONIC POWER

**GMP**

General Microtechnology & Photonics  
Systems for Industry, Research, Telecom & Medicine

## Photonic Power Module

PPM-5



### Key Features

- Complete power delivery system using only fiber optic cable
- Supports 750 to 850 nm and 900 to 1000 nm wavelength range delivering 0.5 to 1 W over 0.5 km of multi-mode fiber
- 5 V DC input, 5 V DC output
- Supports common fiber sizes: 62.5 or 100  $\mu\text{m}$
- Laser power and temperature monitoring interface
- Easy interfacing for designers

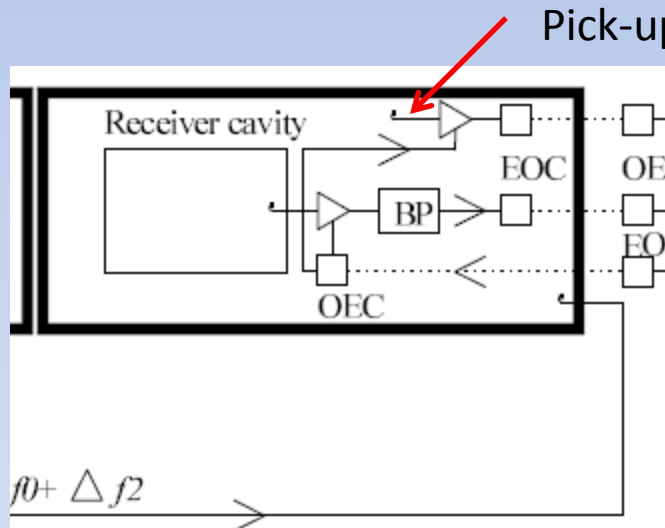
### Applications

- Electronic circuits operating in:
  - high RF, EMI, and magnetic fields
  - high voltage environments

The JDSU PPM-5 Photonic Power Module is an integrated power system that delivers electrical power to another location carried only by light over fiber. This electrically-isolated power source can drive electronics in locations that are hazardous, electrically-noisy, remote, inaccessible, or exposed to extreme weather.

## Two Cavity setup with very high isolation (7)

- The signal at  $f_0 + \Delta f_1$  is the LO (local oscillator signal) for the RF mixers and about 20..30 KHz offset from the carrier  $f_0$  since our the desired intermediate frequency is in the audio range (otherwise we could get too much data for a 2 weeks signal observation).



Pick-up antenna inside shielding box

The remaining signal  $f_0 + \Delta f_2$  is feed directly into the space between the outer shielding box and the actual receiver cavity and if there is any leakage, it will be seen by the PU antenna . This PU antenna will also see , if there is leakage , signals at  $f_0$  (which would be a veto condition) and possibly at  $f_3$  (can be accepted if there is no  $f_3$  signal form the receiver cavity)



## Two Cavity setup with very high isolation (8)

- The frequency locked signal generators (locked to  $f_0$ ) have to exhibit a very low **relative** phase noise in particular the LO (local oscillator for down-mixing).
- This may be accomplished down to the milli-Hz range by means of PLLs (phase locked loop) circuits but there is a question mark about achieving micro-Hz
- For relative phase noise in the micro Hz range the use of a **SERRODYNE** Modulator is proposed
- A serrodyne modulator is displacing a given frequency spectrum (or line) by just adding a constant phase shift per unit of time i.e 360 deg in very small steps in each time interval of 50 microseconds for 20 KHz offset. This frequency displacement is insensitive to frequency variations of  $f_0$  and could also be used for tracking some given (and ramped) accelerator RF.

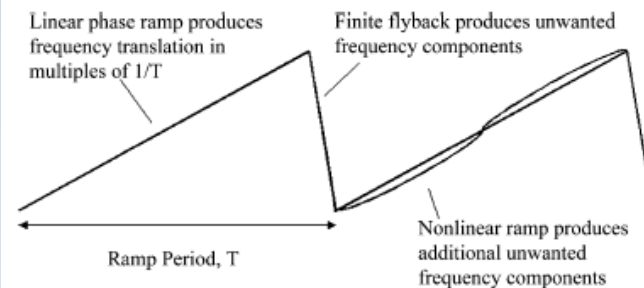
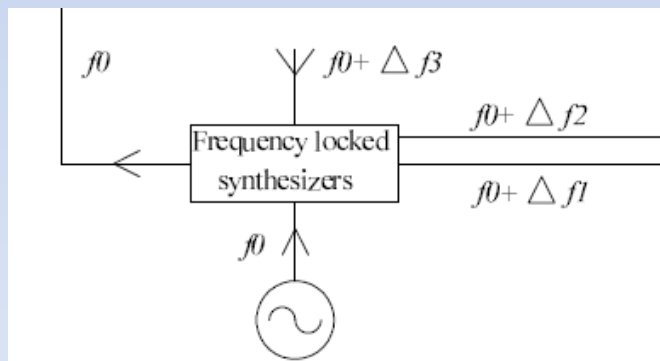


Fig. 1. Important characteristics of serrodyne modulation.

From: S. McDermitt,  
F.Buchholtz: RF  
frequency shifting  
via...  
IEEE-MTT Vol 53,  
No12,Dec 2005,  
page 3782-3787

# A milli-Hz range observation bandwidth set-up (1)

- A simple test experiment has been performed with standard RF instrumentation in order to crosscheck feasibility of very low observation bandwidth implementation (milli Hz bandwidth via FFT on 1000 s time trace)
- As a reminder: the available thermal noise power density at ambient temperature is  $-174$  dBm/Hz or (or  $4 \cdot 10^{-21}$  Watt/Hz) and accordingly =  $-204$  dBm/milliHz, or  $-224$  dBm/milliHz @3 K =  $4 \cdot 10^{-26}$  Watt/mHz @3 K.
- Thus by reducing the observation bandwidth down to the milli- and microHz range we can gain a lot on thermal noise background reduction, provided that the “frequency” of our axions is defined with the same resolution.(i.e. RF cavity generation and receiver concept)

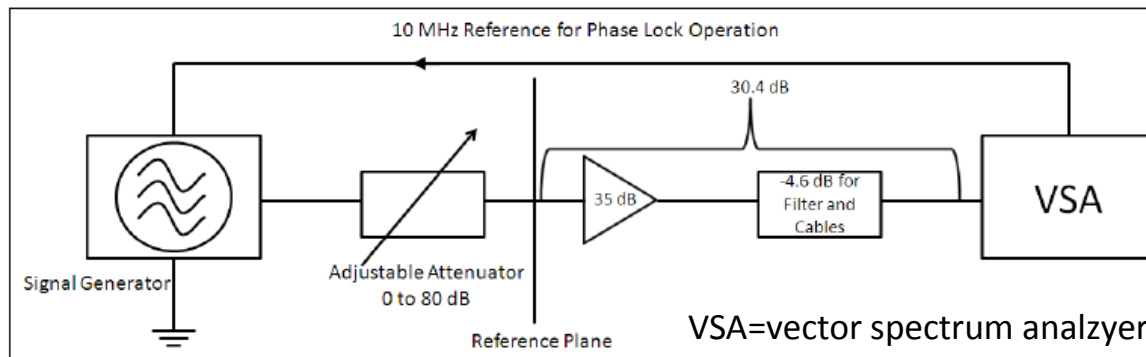


Figure 1: Schematic diagram of the test setup

From: Caspers et al.  
Demonstration of  $10^{-22}$  Watt  
signal detection methods in  
the microwave range at  
ambient temperatures.  
CERN BE-Note 2009-026  
July 2009

# A milli-Hz range observation bandwidth set-up (2)

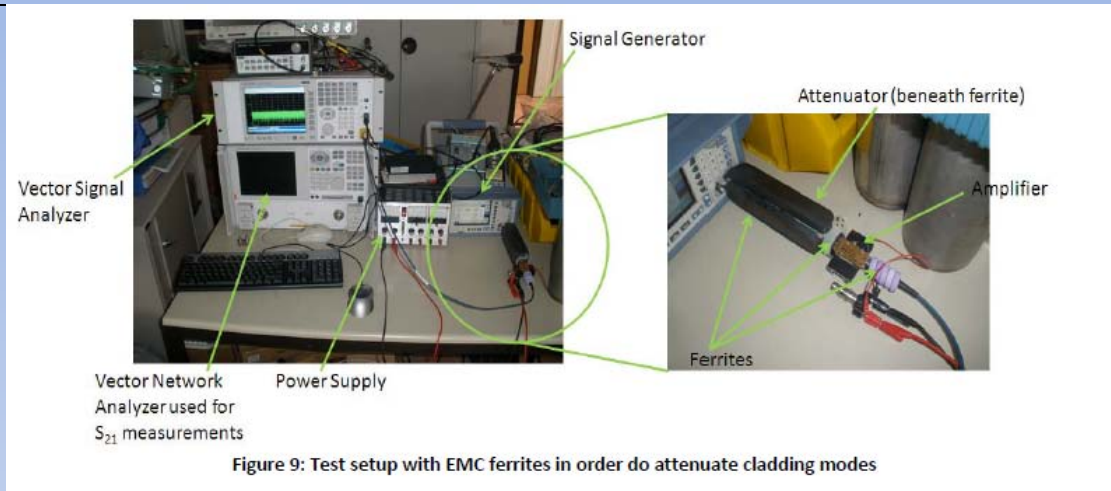
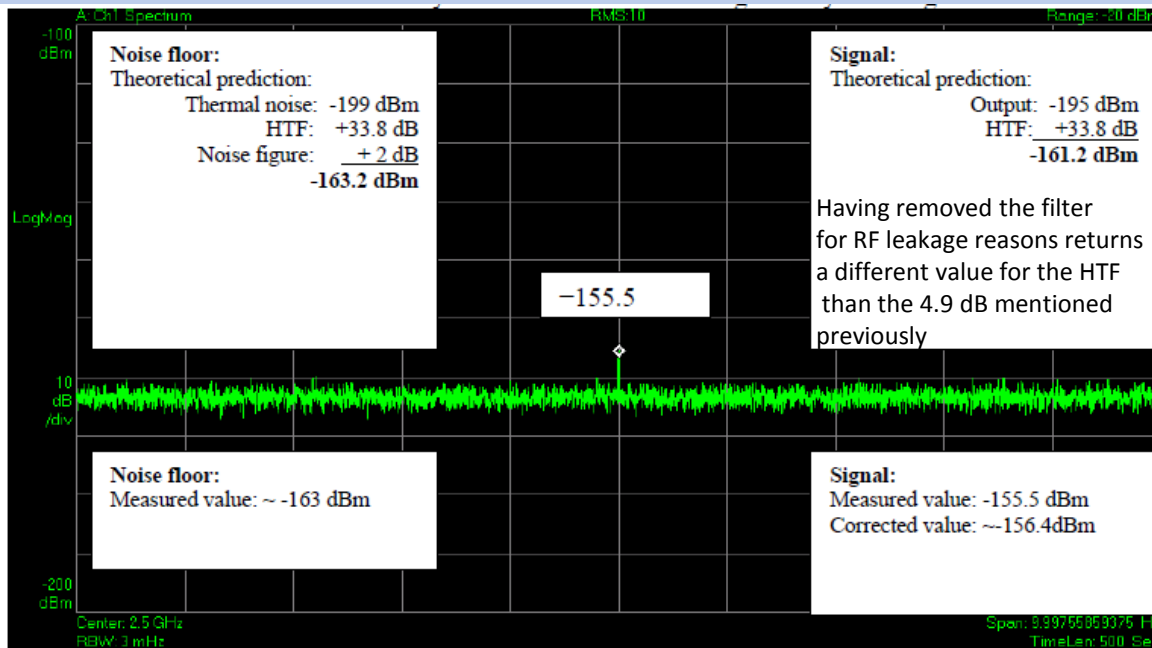


Photo of the very simple test setup (from CERN BE-Note 2009-026)



Measured results  
CERN BE-Note 2009-026

Note that the number shown on the display are to be corrected by the gain (33.8 dB) of the preamplifier at its noise figure (2 dB)

Those thermal noise floor is very close to the expected value, while the measured RF signal is about 5 dB higher due to RF leakage in the attenuator and cable chain

HTF= hardware transfer function

## Discussion of narrowband CW measurements and high peak power pulse methods in terms of RF leakage control and thermal noise background

- The “box in the box “concept appears well suited in particular on the receiver side for getting more than 200 dB electromagnetic isolation.
- The proposed method of online control and verification (using the auxiliary signals discussed above) should in principle be generally applicable.
- However there are some basic differences and question marks:
  - How far can we extend the classical approach (used in this talk) when we are going to look for individual microwave photons generated by axions in the receiver cavity ?
  - On the receiver side we would try to get in both cases the lowest possible front end noise temperature (in the order of 1 deg Kelvin)
  - For the high peak power concept, time domain noise gating (used in beam observation since about 1990 and these days in LHC and FNAL Schottky observation) is certainly applicable .
  - The narrowband method would probably be better suited, if one uses existing accelerator RF power systems (in parasitic mode) and looks for invisible photons (no magnetic field required in transmitter cavity)
  - The narrowband method is probably not very efficient for cosmic axion searches, since the spectrum and spectral distribution of the incoming axions are not well defined.
  - As a general comment: In radar systems the target detection probability is proportional to the average transmitter power and not to its peak power

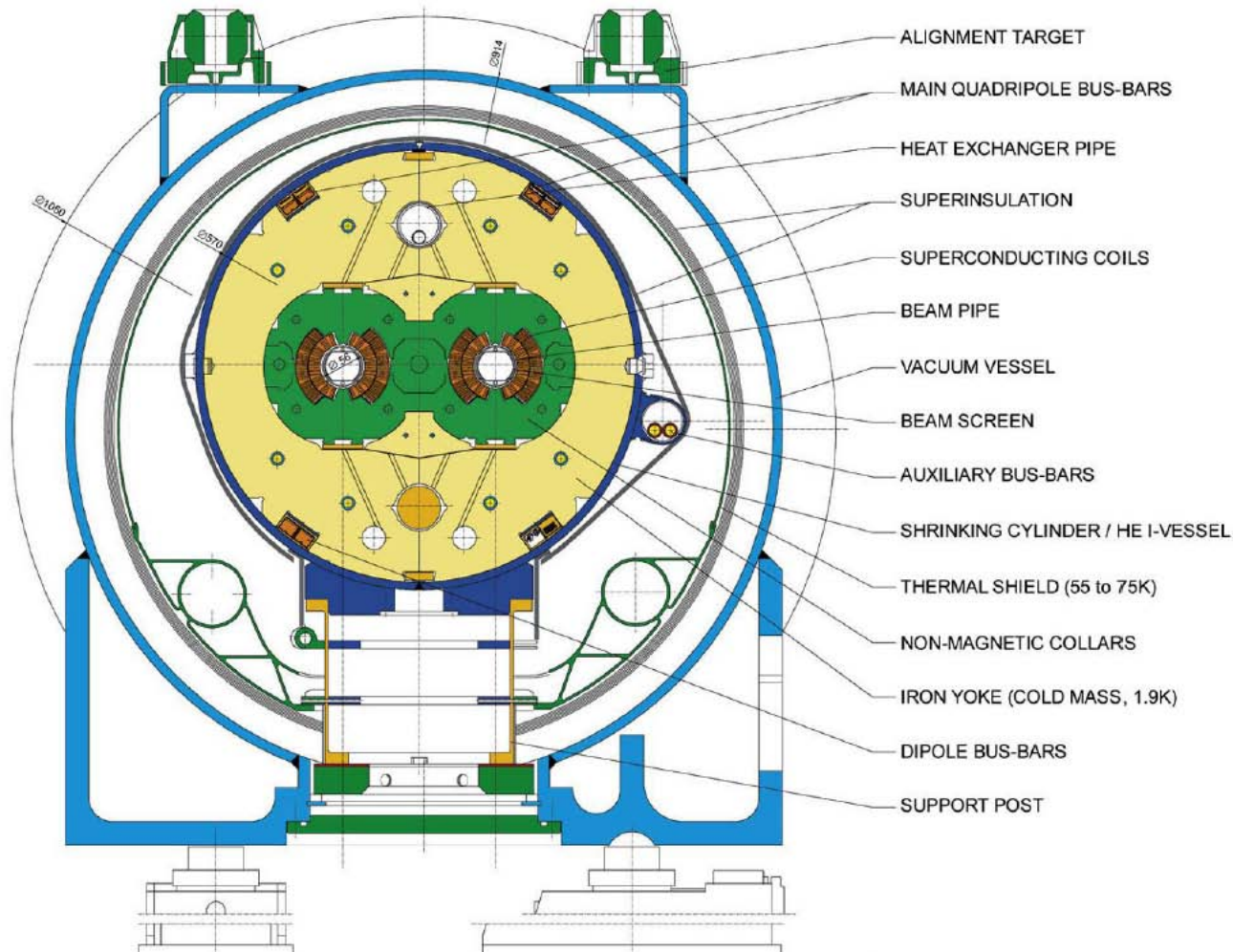
## Rectangular waveguide $TE_{10n}$ resonator in a LHC magnet (1)

- So far, much of the discussion over the last years on axion emitter and receiver cavities has been focused on single mode type cavities (e.g.  $TM_{010}$  mode in a pillbox and a solenoid magnet around)
- Essentially we are aiming for a situation where the RF electric field is parallel to the DC magnetic field over a volume as large as possible.
- When going to higher frequencies with single mode cavities the volume is getting inevitably smaller and thus also the receiver cross-section and sensitivity for a given distance between emitter and receiver cavity.
- For a single mode cavity we cannot expect a very strong directionality in the “antenna diagram “ since the maximum linear dimension of the radiating volume (and accordingly by reciprocity for the receiver antenna) is comparable to a single free space wavelength
- Higher order mode (with a well defined mode pattern) radiating and receiving structures should exhibit an axion radiation pattern with much better “antenna directivity” as compared to an “elementary dipole”
- Why not use the a  $TE_{10}$  mode waveguide in the bore of an LHC Magnet?

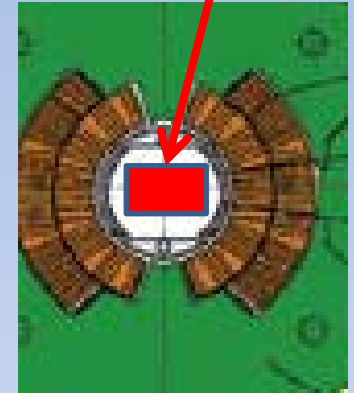
# Rectangular waveguide $TE_{10n}$ resonator in a LHC magnet (2)

## LHC DIPOLE : STANDARD CROSS-SECTION

CERN AC/DI/MM - HE107 - 30 04 1999



$TE_{10}$  waveguide

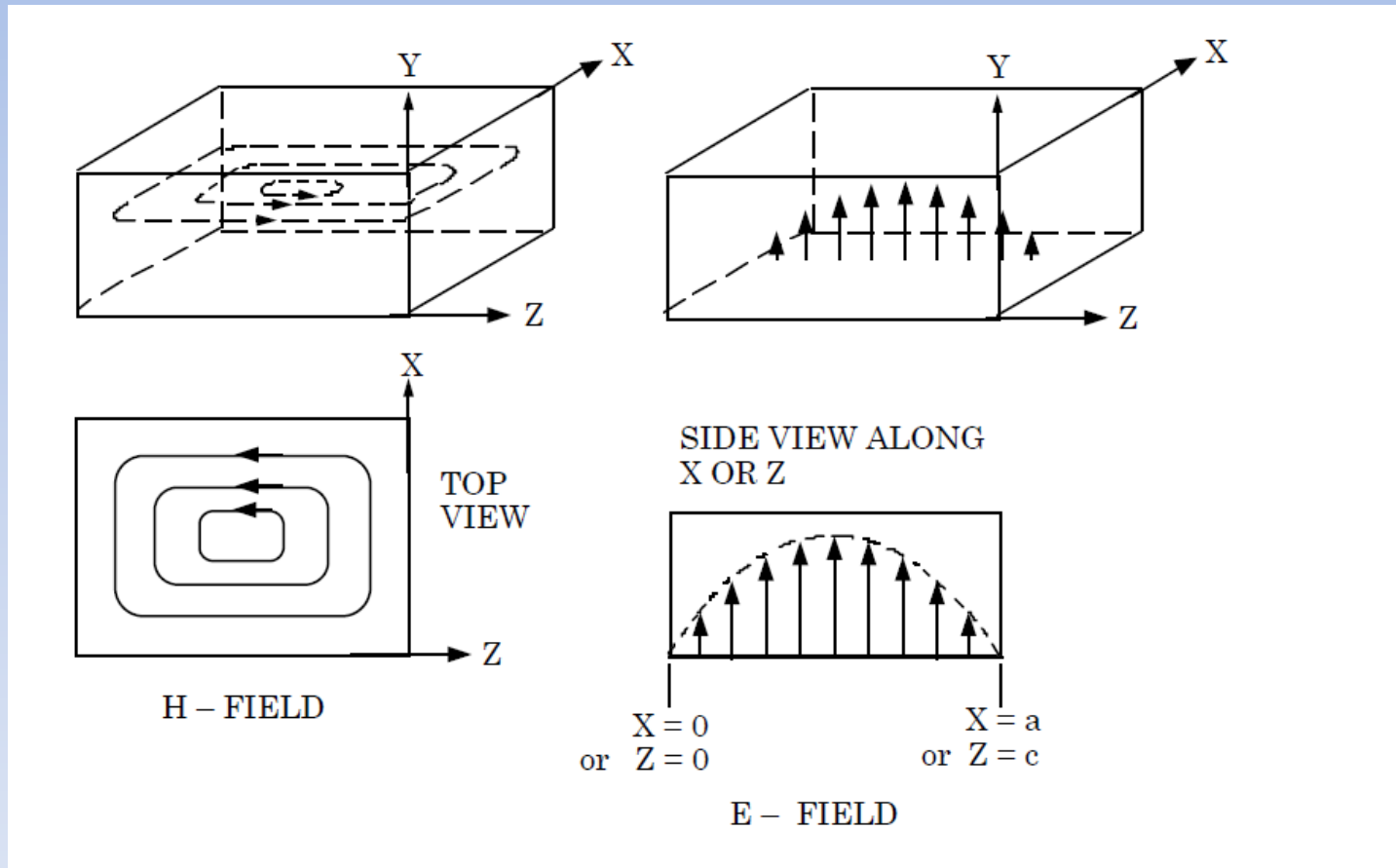


LHC dipole magnet  
Cross-sections and  
proposed position  
and orientation of a  
 $TE_{10}$  waveguide  
in the "beampipe"

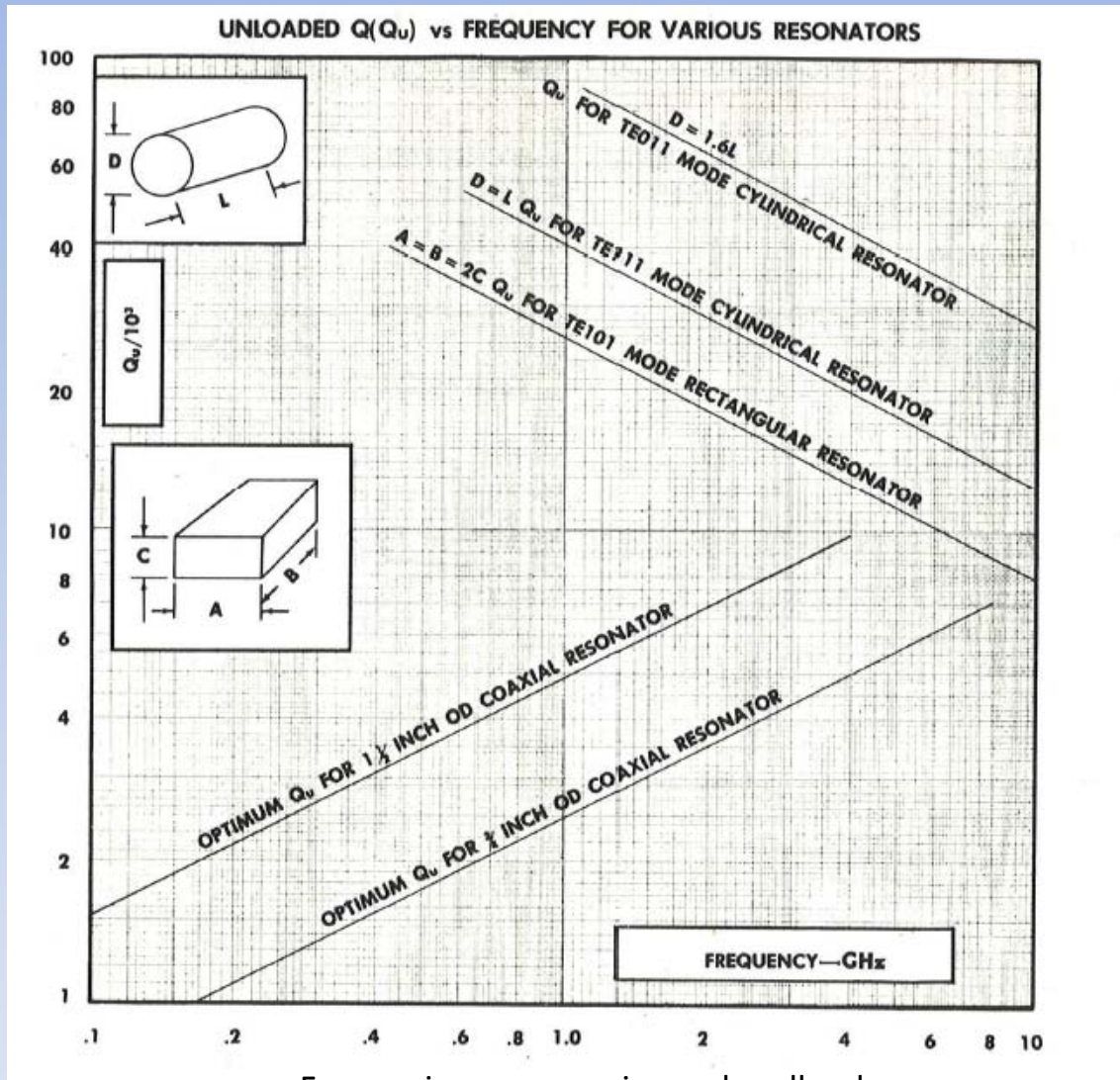


# Rectangular waveguide $TE_{10n}$ resonator in a LHC magnet (3)

Just as a reminder : the  $TE_{101}$  mode pattern in a rectangular waveguide  
For the waveguide in the LHC magnet,  $z$  would be along the beam axis  
and  $y$  in the direction of the static magnetic field (up to 8 Tesla)



# Rectangular waveguide $TE_{10n}$ resonator in a LHC magnet (4)



From: microwave engineers handbook

Here we have the  $Q$  values of different types of waveguide and coaxial line resonators as a function of frequency. For the  $TE_{101}$  resonator (rectangular waveguide with aspect ratio 2/1) we can assume an unloaded  $Q$  value of about 8000 for 10 GHz (X-band) at room temperature and no magnetic field. At cryo temp assuming copper with a RRR value of 100 the  $Q$  would be 10 times higher, but due to the magneto-resistance in the end probably just better by a factor of 3..5.



# Rectangular waveguide TE<sub>10n</sub> resonator in a LHC magnet (5)

Comparison of “tallguide” and normal rectangular waveguide attenuation

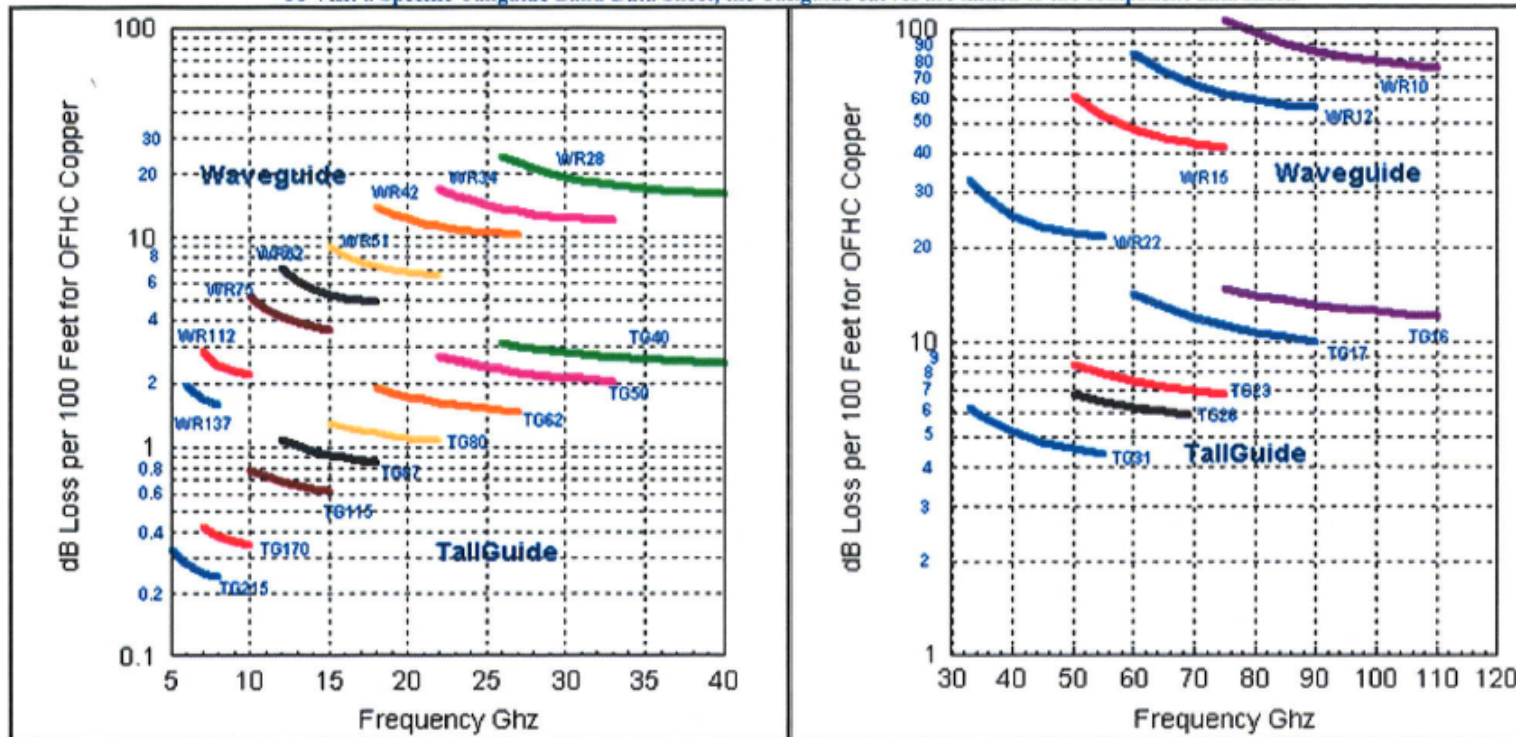
Remark: typical waveguide loss (silver) WR 75 (X-band) =0.15 dB/meter @11 GHz

This corresponds to 2.25 dB along the LHC magnet or nearly 5 dB for a round trip



## Transmission Loss Tallguide® vs. Waveguide for Various Frequency Bands 5 to 110 GHz

To Visit a Specific Tallguide Band Data Sheet, the Tallguide curves are linked to the component data sheet.



# Rectangular waveguide TE<sub>10n</sub> resonator in a LHC magnet (6)

EIA designation (Standard US and /RG number)	RCSC Designation (Standard UK)	Band	Inside Dimensions inches	Outside Dimensions inches (typ)	Standard Freq Range, GHz	Cutoff Freq GHz, Source #1, (Source #2)	Loss per foot Low end - High end of waveguide band	Power Handling Low to High freq  MW=Megawatts, kW=Kilowatts
WR650 /RG69	WG 6	-	6.50, 3.25	6.66, 3.41	1.12 to 1.70	? (0.91)	-	-
WR430 /RG104	WG 8	-	4.30, 2.15	4.46, 2.31	1.70 to 2.60	? (1.37)	-	-
WR340	WG 9A	-	3.40, 1.70	3.56, 1.86	2.10 to 3.00	? (1.6)	-	-
WR284 /RG48	WG 10	-	2.84, 1.34	3.00, 1.50	2.60 to 3.95	? (2.08)	-	2.2 - 3.2 MW
WR229	WG11A	-	2.29, 1.145	2.418, 1.273	3.30 to 4.90	? (2.58)	-	1.6 - 2.2 MW
WR187 /RG49	WG12	-	1.872, 0.872	2.000, 1.000	3.95 to 5.85	? (3.16)	-	1.4 - 2.0 MW
WR159	WG13	-	1.590, 0.795	1.718, 0.923	4.90 to 7.05	? (3.71)	-	0.79 - 1.0 MW
WR137 /RG50	WG14	-	1.372, 0.622	1.500, 0.750	5.85 to 8.20	? (4.31)	-	560 - 710 kW
WR112 /RG51	WG15		1.122, 0.497	1.250, 0.625	7.05 to 10.00	? (5.27)	-	350 - 460 kW
WR90 /RG52	WG16	X	0.900, 0.400	1.000, 0.500	8.20 to 12.4	? (6.56)	-	200 - 290 kW
			0.750,	0.850,	10.0 to			

The table on the left shows rectangular waveguide dimensions from L-band up to X-band (8.2 to 12.4 GHz). Note the CW power handling capability of an X-band waveguide **in air** which is roughly 200 kW. A X-band waveguide would nicely fit into the “beamscreen” of an LHC magnet. For higher frequencies i.e. around 100 GHz one may consider A PACKAGE of say up 20 waveguide in parallel

# Rectangular waveguide TE<sub>10n</sub> resonator in a LHC magnet (7)

WR75	WG17	-	0.375	0.475	15.0	?(7.87)	-	170 - 230 kW
WR62 /RG91	WG18	Ku	0.622, 0.311	0.702, 0.391	12.4 to 18.0	9.50 (9.52)	-	120 - 160 kW
WR51	WG19	-	0.510, 0.255	0.590, 0.335	15.0 to 22.0	? (11.57)	-	80 - 107 kW
WR42 /RG53	WG20	K	0.420, 0.170	0.500, 0.250	18.0 to 26.5	14.08 (14.05)	0.26 - 0.20 dB	43 - 58 kW one source
WR28 /RG96	WG22	Ka	0.280, 0.140	0.360, 0.220	26.5 to 40.0	21.08 (21.08)	0.44 - 0.30 dB	96 - 146 kW
WR22 /RG97	WG23	Q	0.224, 0.112	0.304, 0.192	33.0 to 50.0	26.34 (26.82)	0.62 - 0.42 dB	64 - 97 kW
WR19	WG24	U	0.188, 0.094	0.268, 0.174	40.0 to 60.0	31.36 (31.06, 30.69)	0.77 - 0.54 dB	48 - 70 kW
WR15 /RG98	WG 25	V	0.148, 0.074	0.228, 0.154	50.0 to 75.0	39.87 (39.90, 39.34)	0.10 - 0.80 dB	30 - 40 kW
WR12 /RG99	WG 26	E	0.122, 0.061	0.202, 0.141	60.0 to 90.0	48.35 (48.40, 49.18)	1.8 - 1.0 dB	? kW
WR10	WG 27	W	0.100, 0.050	0.180, 0.130	75.0 to 110.0	59.01 (58.85)	2.0 - 1.4 dB	14 - 25 kW
WR8	WG 28	F	0.080, 0.040	0.160, 0.120	90.0 to 140.0	73.77 (73.84)	3.0 - 2.0 dB	8.8 - 13 kW
WR6	WG ?	D	0.065, 0.0325	0.145, 0.112	110 to 170	90.79 (90.48, 84.31)	3.8 - 3.0 dB	5.9 - 9.3 kW
WR5	WG ?	G	0.0510, 0.0255	0.131, 0.105	140 to 220	115.7 (118.03)	6.1 - 3.8 dB	3.7 - 6.1 kW
WR3	WG ?	Y	0.034, 0.0170	0.114, 0.097	220 to 325	196.71 (196.71)	10.0 - 7.0 dB	1.9 - 2.6 kW

The losses for (non overmoded) metallic waveguides increase dramatically towards higher frequencies and accordingly the power handling capability decreases.

One can gain about a factor of 10 in losses by using overmoded waveguides (“tallguide”). As an alternative above 50 GHz dielectric waveguides with a metallic shielding become competitive

In a way a “optical fiber”  
In the microwave range

# Rectangular waveguide TE<sub>10n</sub> resonator in a LHC magnet (8)

## A WARM BORE ANTICRYOSTAT FOR SERIES MAGNETIC MEASUREMENTS OF LHC SUPERCONDUCTING DIPOLE AND SHORT-STRAIGHT-SECTION MAGNETS.

Presented at the 2003 Cryogenic Engineering Conference and International Cryogenic Materials Conference  
CEC/ICMC 2003  
22-26 September 2003, Anchorage, Alaska

O. Dunkel, P. Legrand and P. Sievers

CERN, AT Division,  
CH-1211 Geneva 23, Switzerland

All LHC twin aperture magnets will be tested under operating conditions to verify their performance. The field measurement equipment works at ambient temperature and pressure. Each magnet is therefore equipped with two warm bore anticryostats. As a consequence a total of nearly 80 anticryostats of different lengths have to be assembled, handled and serviced during the test period. Two main constraints determine the frame for the design of these anticryostats: inside a given beam pipe aperture of 50 mm kept at 1.9 K, a warm bore aperture of 40 mm must provide the highest possible mechanical stability and robustness for numerous mounting cycles as well as the lowest possible heat losses towards the cryogenic system. In addition, compatibility with high magnetic fields and an insulation vacuum of about  $10^{-7}$  mbar have to be maintained. This paper describes how a satisfactory mechanical stability as well as heat losses in the order of 0.8 W/m are achieved with a design based on very careful space and material optimization. Other aspects like assembly, installation, thermal behavior and temperature control during the operation are described.

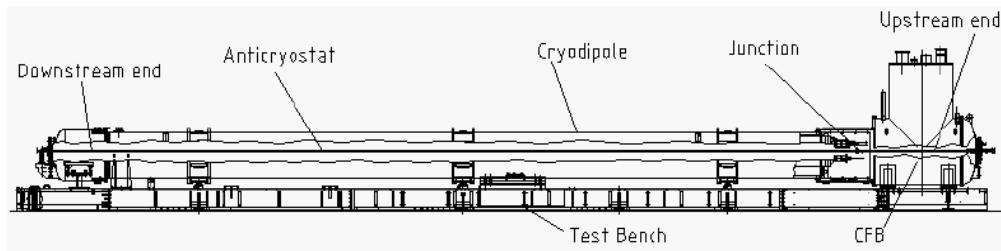


FIGURE 2. Layout of a cold test bench for dipole magnets equipped with anticryostats.

## The ANTI-CRYOSTAT

We may consider using the anti-cryostat for the axion transmitter part. Then we are no longer restricted by the cryo power dissipation limit of 2 Watt per meter of the LHC main dipole beam screen, but we could apply water cooling along the 15 meter long waveguide and possibly dissipate 10 KW maybe even 100 KW CW. Of course this does not make sense for the receiver cavity (low noise temperature required)



# Rectangular waveguide TE<sub>10n</sub> resonator in a LHC magnet (9)

## A WARM BORE ANTICRYOSTAT FOR SERIES MAGNETIC MEASUREMENTS OF LHC SUPERCONDUCTING DIPOLE AND SHORT-STRAIGHT-SECTION MAGNETS.

Presented at the 2003 Cryogenic Engineering Conference and International Cryogenic Materials Conference  
CEC/ICMC 2003  
22-26 September 2003, Anchorage, Alaska

O. Dunkel, P. Legrand and P. Sievers

CERN, AT Division,  
CH-1211 Geneva 23, Switzerland

All LHC twin aperture magnets will be tested under operating conditions to verify their performance. The field measurement equipment works at ambient temperature and pressure. Each magnet is therefore equipped with two warm bore anticryostats. As a consequence a total of nearly 80 anticryostats of different lengths have to be assembled, handled and serviced during the test period. Two main constraints determine the frame for the design of these anticryostats: inside a given beam pipe aperture of 50 mm kept at 1.9 K, a warm bore aperture of 40 mm must provide the highest possible mechanical stability and robustness for numerous mounting cycles as well as the lowest possible heat losses towards the cryogenic system. In addition, compatibility with high magnetic fields and an insulation vacuum of about  $10^{-7}$  mbar have to be maintained. This paper describes how a satisfactory mechanical stability as well as heat losses in the order of 0.8 W/m are achieved with a design based on very careful space and material optimization. Other aspects like assembly, installation, thermal behavior and temperature control during the operation are described.

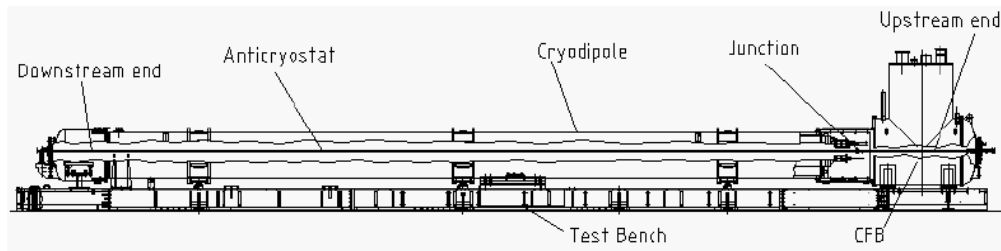
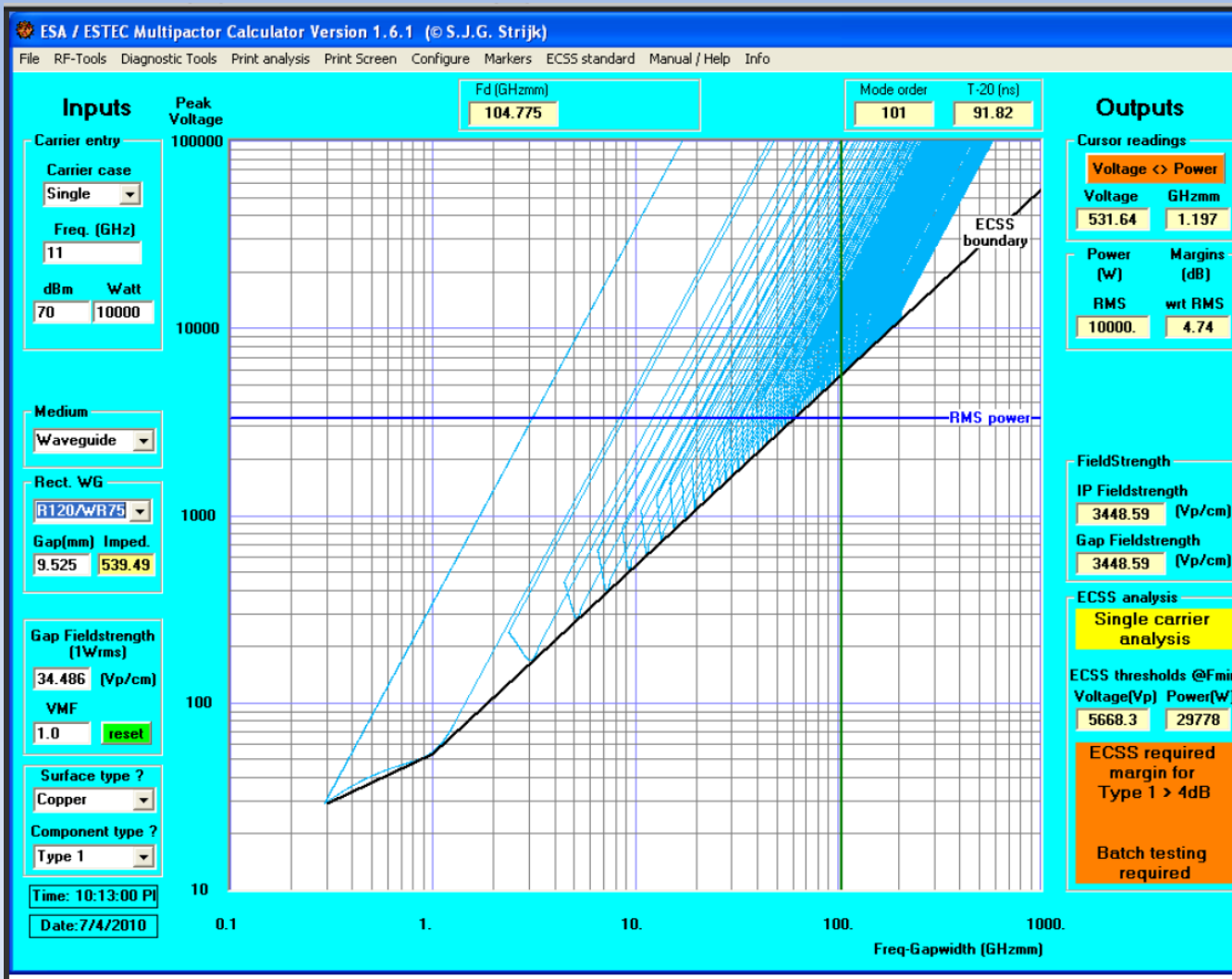


FIGURE 2. Layout of a cold test bench for dipole magnets equipped with anticryostats.

## The ANTI-CRYOSTAT

We may consider using the anti-cryostat for the axion transmitter part. Then we are no longer restricted by the cryo power dissipation limit of 2 Watt per meter of the LHC main dipole beam screen, but we could apply water cooling along the 15 meter long waveguide and possibly dissipate 10 KW maybe even 100 KW CW. Of course this does not make sense for the receiver cavity (low noise temperature required)

# Rectangular waveguide TE<sub>10n</sub> resonator in a LHC magnet (10)



Working in air or vacuum on the (warm) transmitter side?  
Multipacting ?!

A quick analysis with the ESA multipactor calculator shows that in vacuum and without magnetic field we are already for 10 KW power from the generator in a critical region (but to be re-checked with magnetic field)

# Axion radiation patterns-standing wave structure in a waveguide (1)

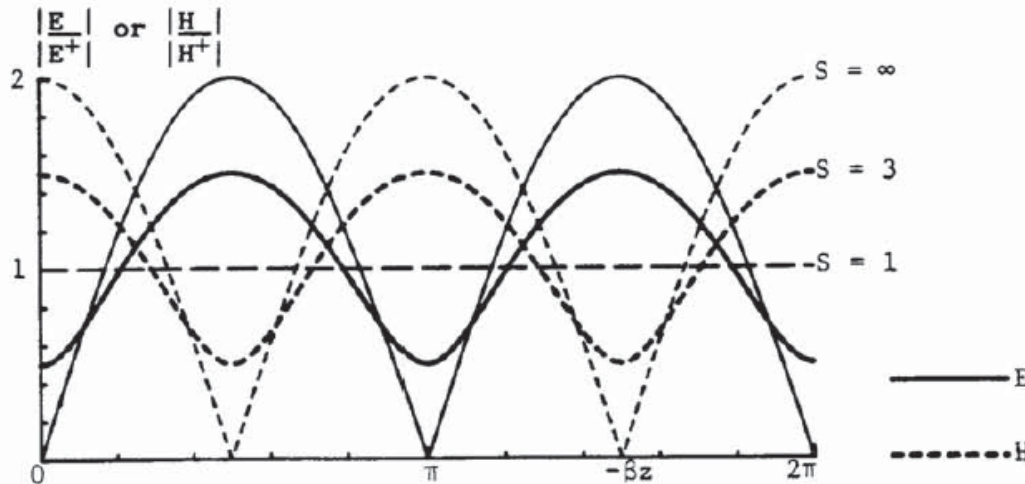
As a reminder: Amplitude variation along a transmission line (coax or waveguide)

For simplicity's sake we assume that the attenuation  $\alpha$  is negligible.

$$\frac{|E|^2}{|E^+|^2} = 1 + |\rho|^2 + 2|\rho|\cos(2\beta z + \phi_o) = (1 - |\rho|)^2 + 4|\rho|\cos^2\left(\beta z + \frac{\phi_o}{2}\right)$$

$$\frac{|H|^2}{|H^+|^2} = 1 + |\rho|^2 - 2|\rho|\cos(2\beta z + \phi_o) = (1 - |\rho|)^2 + 4|\rho|\sin^2\left(\beta z + \frac{\phi_o}{2}\right)$$

$|E|$  is maximum when  $|H|$  is minimum, and vice versa



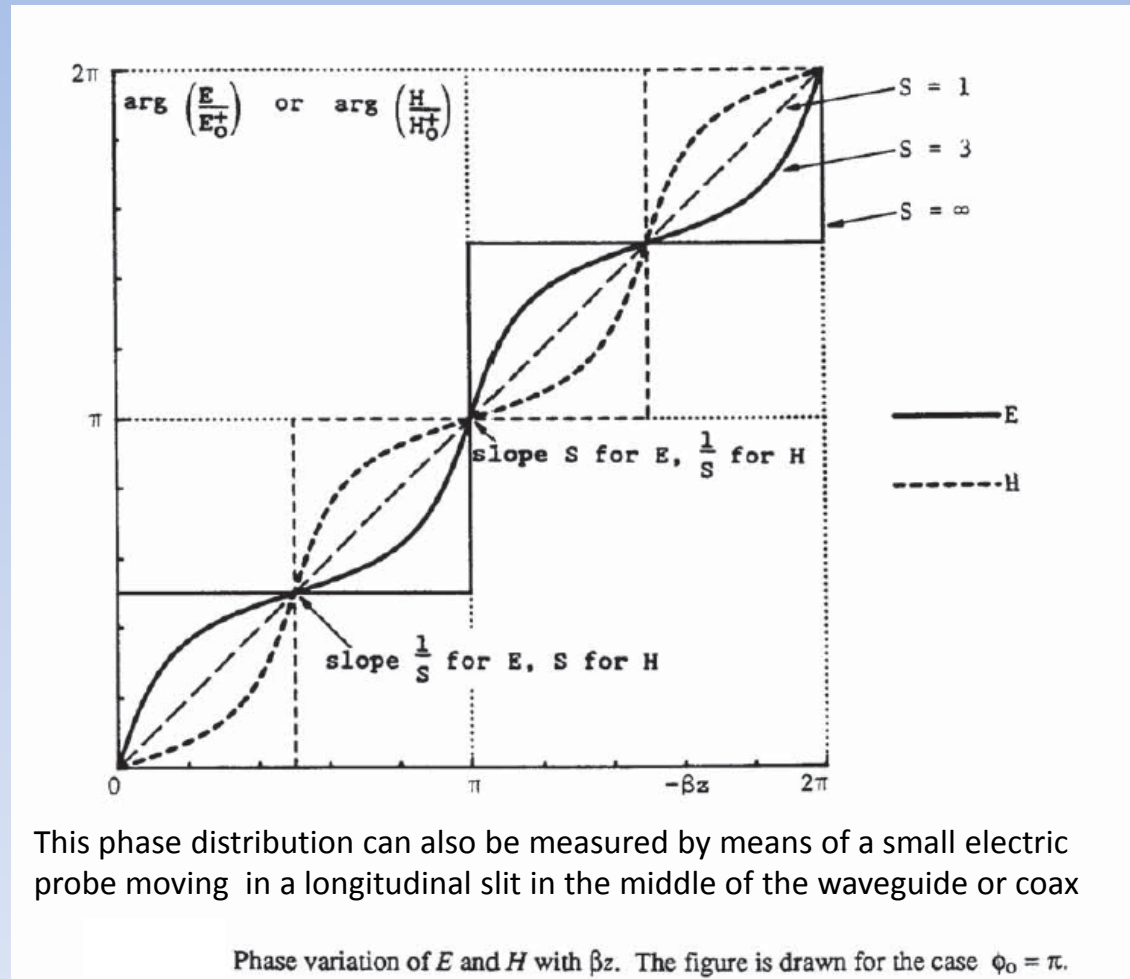
Amplitude variation of  $E$  and  $H$  with  $\beta z$ . In the figure, for  $S = \infty$  we have taken  $\phi_o = \pi$  (i.e.  $\rho_o = -1$ )

From: G. Dome  
Basic RF Theory,  
waveguide and cavities  
CERN RF Accelerator School  
Oxford 1991  
CERN yellow report 92-03

Explanation of symbols  
 $\rho$  = (voltage) reflection coeff.  
 $s$  = Standing wave ratio (SWR)  
or VSWR (voltage standing  
wave ratio)  
For a purely travelling wave we  
have  $s=1$  and for complete  
reflection  $s=\infty$ , the case  $s=3$   
corresponds to a reflection factor  
of 50% in Voltage or 25 % in  
power

# Axion radiation patterns-standing wave structure in a waveguide (2)

As a reminder: phase variation along a transmission line (coax or waveguide)



This phase distribution can also be measured by means of a small electric probe moving in a longitudinal slit in the middle of the waveguide or coax

From: G. Dome  
Basic RF Theory,  
waveguide and cavities  
CERN RF Accelerator School  
Oxford 1991  
CERN yellow report 92-03

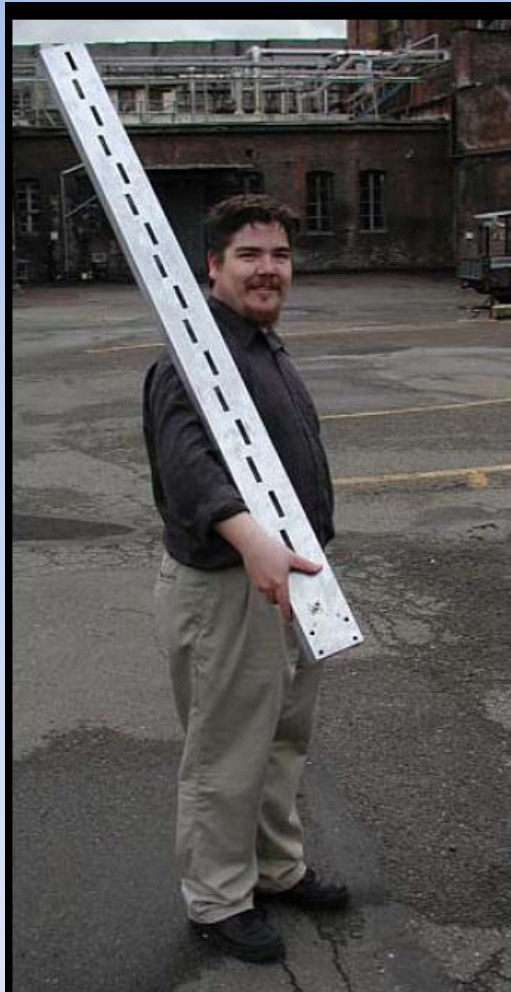
Note that for a purely travelling wave ( $s=1$ ) the phase is just increasing linear with distance, where for total reflection ( $s=\infty$ ) the phase is constant over half a wavelength and we get a phase jump of 180 deg at every half wavelength.

If we use a 15 meter long x-band waveguide as resonator, we may approach the case  $s=3$ .



# Axion radiation patterns-waveguide as phased array antenna (1)

An example for a waveguide slot antenna array



In this example we see a number of slots (not centered, in order to cut through wall currents and thus provide an electric and magnetic polarization of each slot.

This kind of antenna structure (often at higher frequencies than shown here) is widely used in maritime radars but also for final approach landing radar on airports and of course for all kind of military applications. There is a strong analogy to the axion radiation (and reception) pattern.


Such kind of antenna structures can be used in standing and in travelling wave mode

# Axion radiation patterns-waveguide as phased array antenna (2)

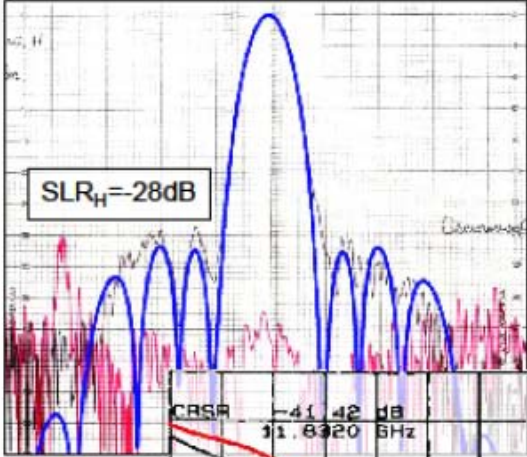
Another example for a slotted waveguide phase array antenna incl the directional diagram

## Low Side Lobe Slotted Waveguide Arrays

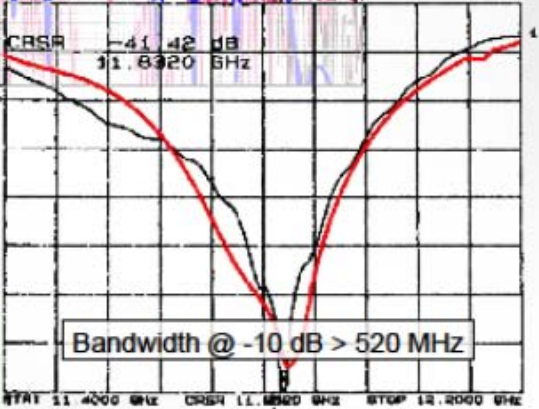
**RF<sub>u</sub>tech**  
a spin-off of the University of Perugia



low side lobe  
X-band slotted wg array



$SLR_H = -28\text{dB}$



Bandwidth @ -10 dB > 520 MHz

CSRR -41.42 dB  
11.8320 GHz

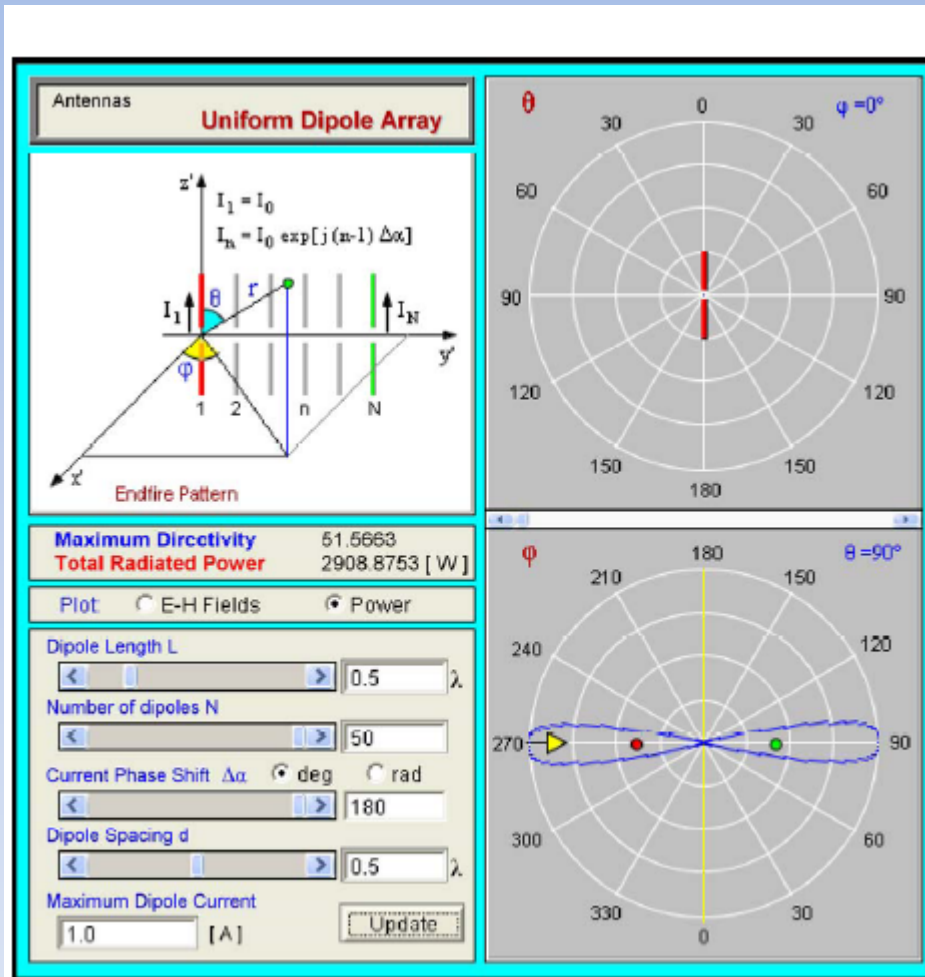
SWAN  
Slotted Waveguide Antennas™  
ANALYSIS AND DESIGN

**Accurate Synthesis  
&  
Short Time to Market**

SWAN-SOFT.com  
Slotted Waveguide Antennas™

# Axion radiation patterns-directional diagrams (1)

Radiation pattern , standing wave mode ,  $v=c$ , 50 dipoles spaced by  $0.5 \lambda$



© Amanogawa, 2010 - All Rights Reserved

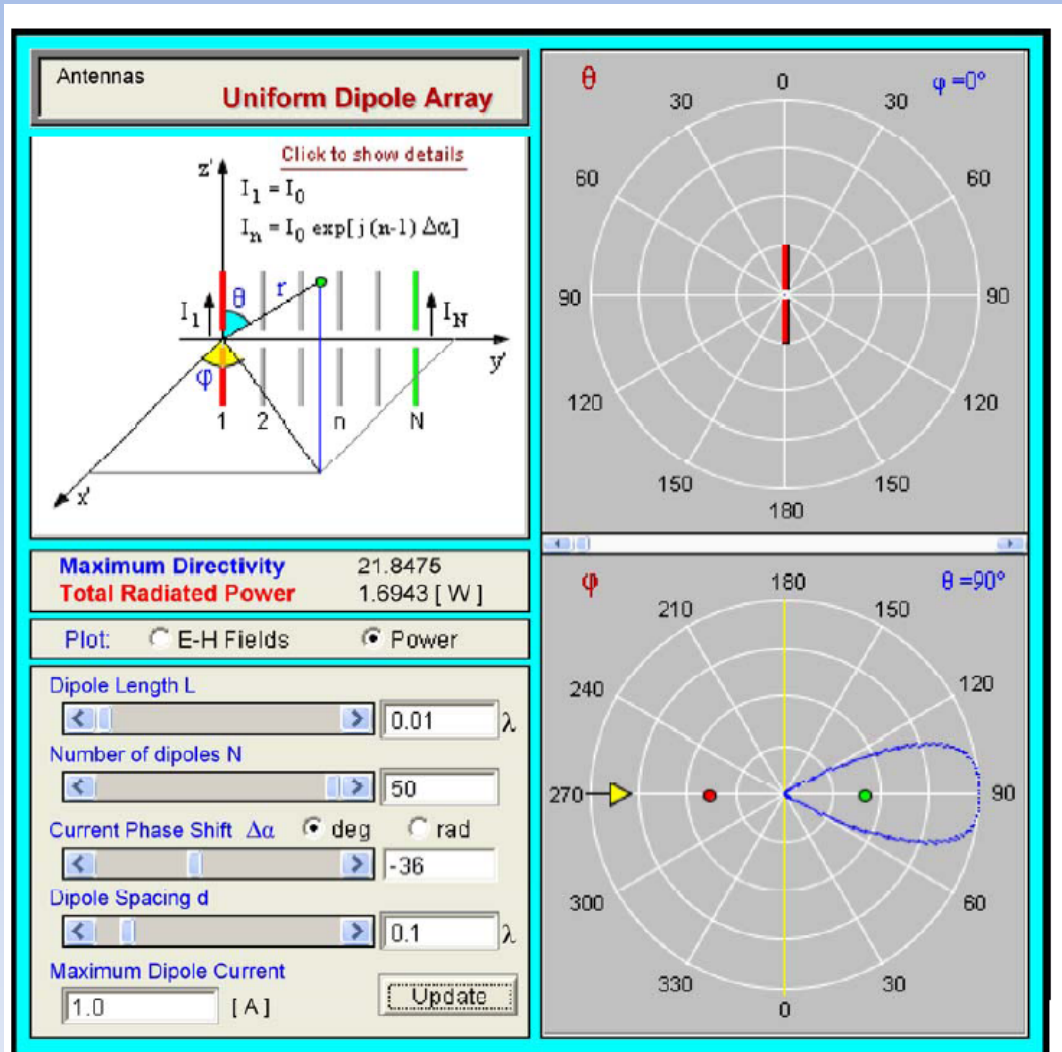
In this example we see nicely the forward and backward radiation lobe ( $\phi=90$  and  $270$  degree respectively) This case corresponds to the standing wave pattern of a laser beam.

The basic law of antenna design:

The radiation characteristic of a group of radiating elements is equal to the characteristic of the group (isotropic radiators) to be multiplied with the characteristic of the individual radiator (e.g. dipole)

# Axion radiation patterns-directional diagrams (2)

Radiation pattern , travelling wave mode ,  $v=c$ , 50 dipoles spaced by  $0.1 \lambda$

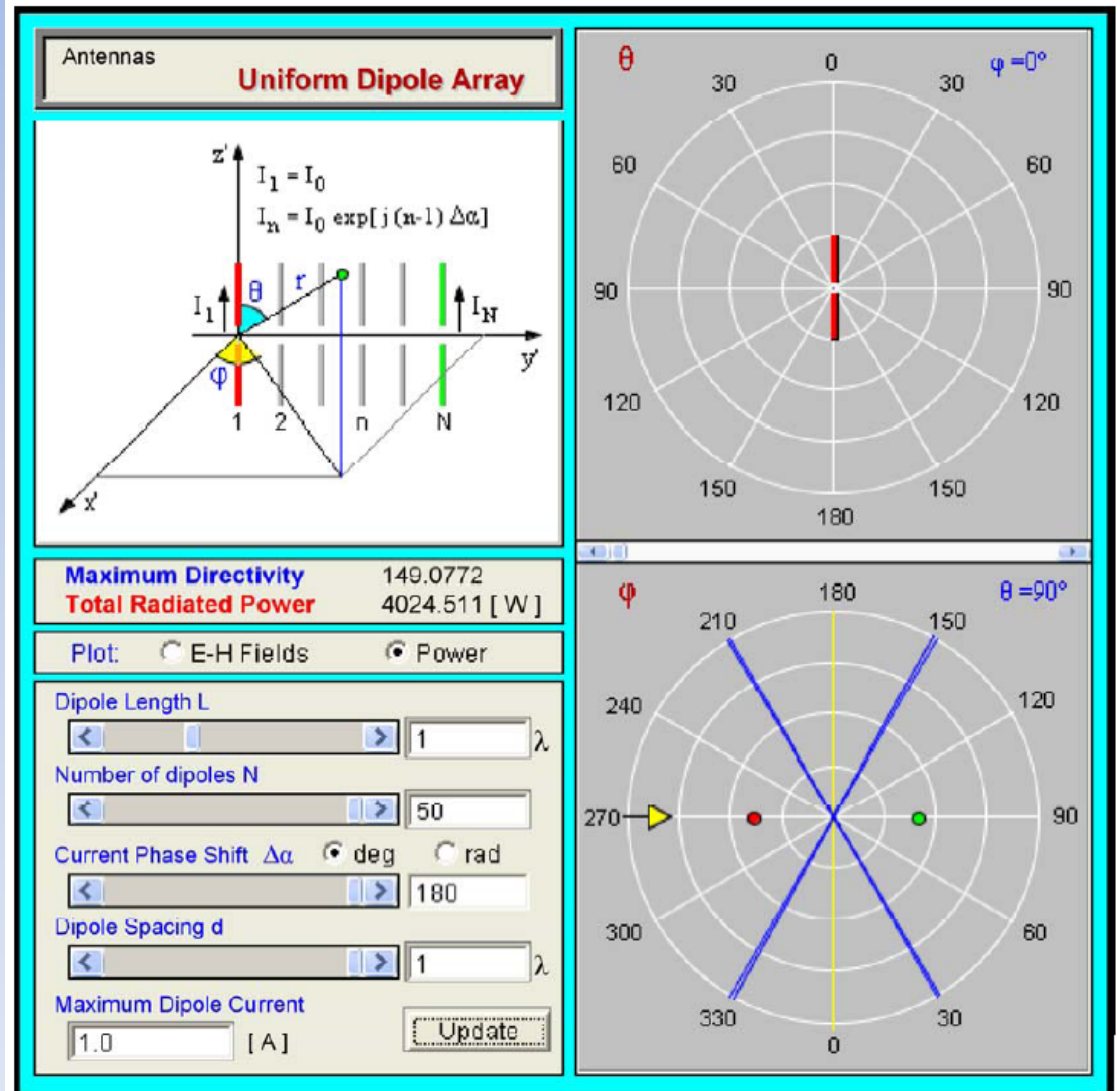


Here we have the radiation pattern of a travelling wave antenna (endfire antenna) Note that the relative spacing of the radiating elements is smaller than in the last slide i.e the antenna is shorter and thus the directional diagram becomes wider This case corresponds to the travelling wave pattern of a laser beam.( $v=c$ )



# Axion radiation patterns-directional diagrams (3)

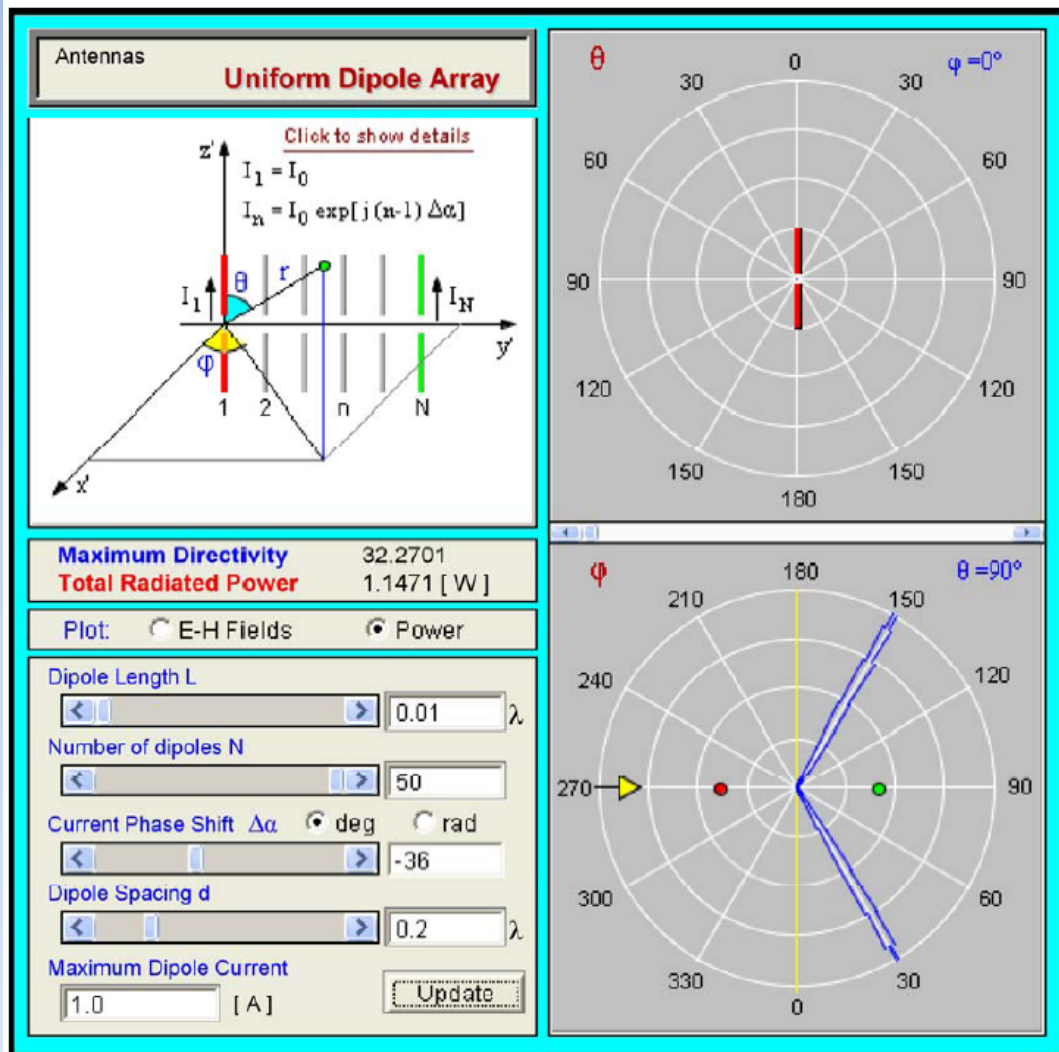
Radiation pattern , standing wave mode ,  $v=2c$ , 50 dipoles spaced by  $0.5 \lambda$



This case is typical for a waveguide slot array antenna or in our case the standing wave pattern in a waveguide where the phase velocity is twice the speed of light. ( $v=2c$ ) Note that the main radiation now is going sideways. The phase velocity in such a waveguide can easily be varied by changing the frequency of the mode.

# Axon radiation patterns-directional diagrams (4)

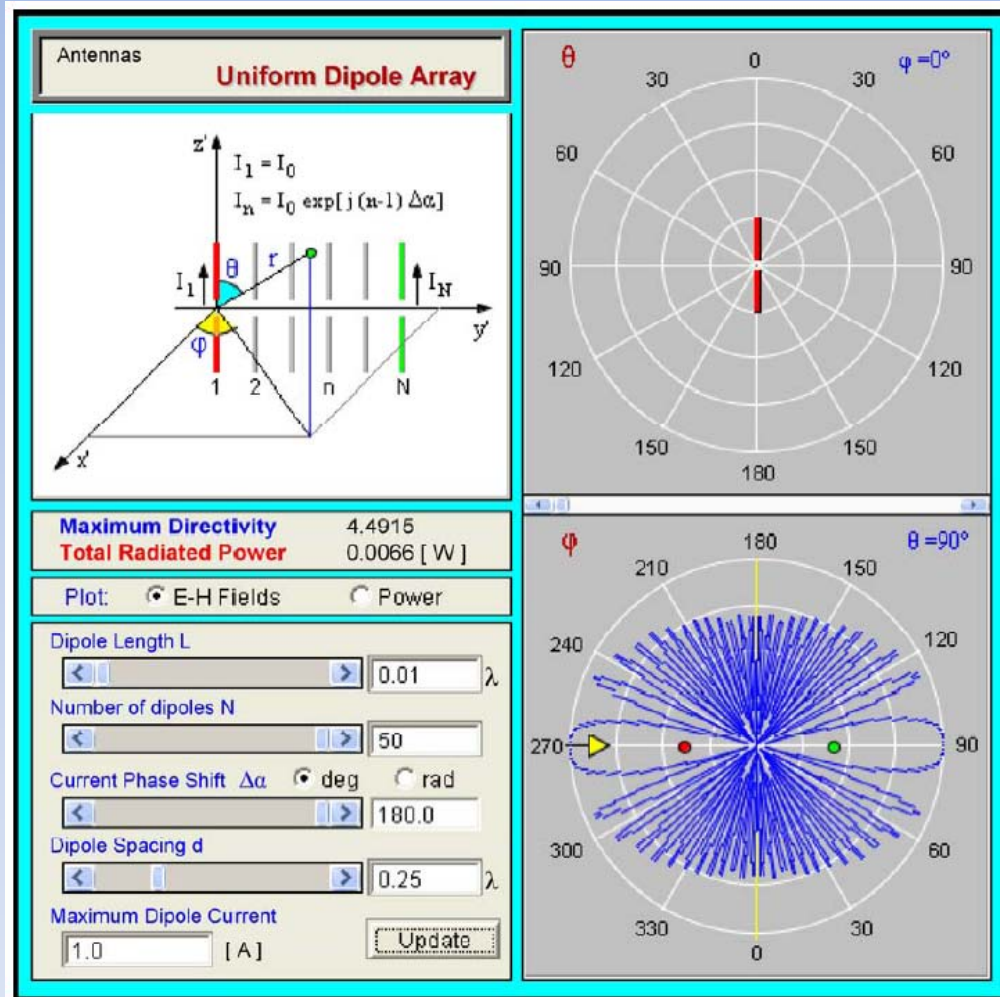
Radiation pattern , travelling wave mode ,  $v=2c$ , 50 dipoles spaced by  $0.2 \lambda$



The result is similar to what was shown in the last slide (main lobes at 30 and 150 deg) but radiation only to one side and the width of the mainlobes is larger since this antenna is shorter than the travelling wave one.

# Axion radiation patterns-directional diagrams (5)

Radiation pattern , standing wave mode ,  $v=0.5c$ , 50 dipoles spaced by  $0.5 \lambda$

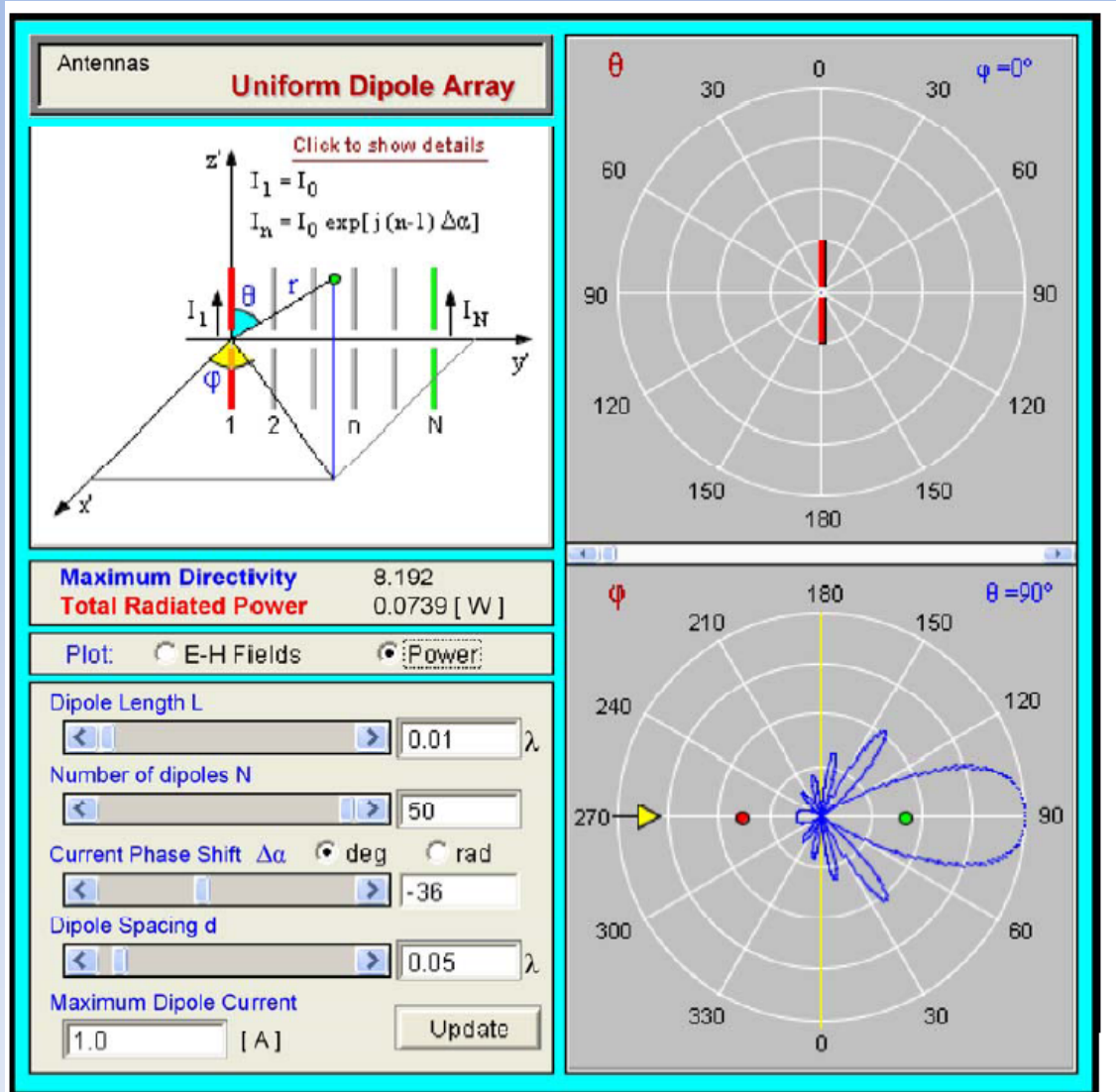


© Amanogawa, 2010 - All Rights Reserved

This radiation pattern has a completely different characteristic ..note the many small sidelobes (here in E/H display and not in power as on the last slides)

# Axion radiation patterns-directional diagrams (6)

Radiation pattern , travelling wave mode ,  $v=0.5c$ , 50 dipoles spaced by  $0.1 \lambda$



We see the main lobe in the same direction as the wave is travelling and there are a few sidelobes (smaller than in last slide since here we are again on the radiated power display). Again the width of the mainlobe is larger since the antenna is significantly shorter than the travelling wave version.



# Conclusion and outlook

- The electromagnetic interference problem , in particular for the receiver cavity is an important issue for microwave axion detection experiments. Here the combination of the “box in the box” concept , together with optical fiber powered diagnostic equipment in the space between the first shielding and the actual cavity, can make a significant contribution.
- Very narrow band signal detection using a say 10 days trace record with about 50 Gigasamples and 24 bit vertical resolution should return via FFT microhz resolution and related thermal noise reduction. A phaselock method to possibly reduce the relative phase noise down the microHz level has been presented and discussed.
- Higher order mode emitter and receiver cavities , possibly in a single or in two LHC magnets were discussed and analyzed in terms of their axion radiation pattern (farfield). Highly directional axion emitter and receiver structures may significantly increase the detection probability.

# Acknowledgements

- The author would like to thank the CERN AB dept management and in particular the AB-RF group for support as well as Steve Myers and R. Heuer for encouragement.
- Many thanks to A. Ringwald and J. Jäckel for a large number of hints and inspiring discussions and K. Zioutas for having brought the right people in the right moment together as well as haven given very helpful comments